Catalysis Letters Vol. 105, Nos. 1–2, November 2005 (© 2005)
DOI: 10.1007/s10562-005-8004-2

ETS-10 modulation to alumina support and its promotion for hydrodesulfurization

Huifeng Li, Baojian Shen*, Xiaohua Wang, and Shikong Shen

State Key Laboratory of Heavy Oil Processing, the Key Laboratory of Catalysis of CNPC, and Faculty of Chemical Science and Engineering, China University of Petroleum-Beijing, Beijing Changping, 102249 China

Received 4 July 2005; accepted 10 August 2005

A composite support with ETS-10 stabilized in alumina, was firstly developed for hydrodesulfurization (HDS). It can impede inactive nickel spinel formation and favor more polymeric tungsten species formation, which facilitates the promotion effect of nickel on tungsten and leads to increasing activity in HDS of 4,6-DMDBT.

KEY WORDS: Ctitanosilicate; ETS-10; composite support; alumina; Al_2O_3–TiO_2; hydrodesulfurization; metal–support interactions.

1. Introduction

For producing ultra-low-sulfur diesel fuels, various approaches and technologies are emerging [1–3]. And the key to achieve this target is the effective removal of sterically hindered sulfur compounds, such as 4,6-DMDBT, under the inhibiting effect of polyaromatics and nitrogen compounds, which is really a big challenge for the conventional hydrotreating catalyst [4]. Therefore, it is imperative to develop more active and more selective hydrotreating catalysts.

Supports, as one of the major constituent parts of hydrotreating catalysts, play an active role in the catalysis. So far, many materials have been employed as supports to load Mo or W active components promoted by Co or Ni [5–7]. Noticeably, the catalysts supported on the mixed oxides containing titania such as TiO_2–Al_2O_3, TiO_2–SiO_2, show easier reducibility or sulfidability and outstanding activities [6]. Besides, compared with that of pure alumina, the incorporation of acidic molecular sieves can also enhance the activity in hydrodesulfurization (HDS) of such refractory sulfur compounds, due to their acid-catalyzed isomerization and disproportionation into more reactive derivatives. However, the previous work mainly focused on the acidity function of the molecular sieve [5,7], the research on the function of framework elements on hydrotreating catalysts, have not reported yet.

Here we would like to report the first example of ETS-10 incorporated composite support for HDS, prepared by introducing titanosilicate ETS-10 into the alumina matrix. More interestingly, ETS-10 owns mild and tunable acidity to suppress undesired cracking or deactivation through the controllable ion-exchange of Na, K of ETS-10 [8,9]. The aim of our present work is to investigate the effects of the introduction of ETS-10 into alumina matrix, and the impact of its unique titanosilicate framework on metal–support interactions and HDS activity.

* To whom correspondence should be addressed.
E-mail: baojian@cup.edu.cn

2. Experimental

2.1. Composite support preparation

In a typical composite support preparation, ETS-10 synthesized with the hydrothermal method [10] was ion-exchanged with ammonium nitrate solution, followed by filtering and washing with deionized water. To make ammonium-exchanged ETS-10 dispersed uniformly in the alumina matrix, the filter cake was repulped in deionized water. And under vigorous stirring (10,000 rpm) the obtained suspension was added dropwise into the pseudo-boehmite sol, which was prepared with the commercial pseudo-boehmite powders peptized with 5 wt% nitric acid at room temperature for 8 h. Subsequently, the sol mixture was stirred vigorously in a water bath at 348 K until the mixture became viscous paste, then followed by extruding, drying, calcining at 823 K for 5 h. And the obtained composite support was designated AETS, containing the titanium content of 4 wt% (calculated by TiO_2). In the same way, the Al_2O_3–TiO_2 support with the same TiO_2 content as composite support AETS, was prepared by using TiO_2 (anatase) powder, while pure Al_2O_3 support was obtained directly from the acidified pseudo-boehmite sol.

2.2. Catalyst preparation

The catalysts NiW/AETS, NiW/Al_2O_3–TiO_2 and NiW/Al_2O_3 with the loading of 4 wt% NiO and 27 wt%

1011-372X/05/1100–0047/0 © 2005 Springer Science+Business Media, Inc.

WO_3, were prepared by pore volume co-impregnation method with an aqueous solution of ammonium metatungstate and nickel nitrate. Prior to use, all the samples were dried overnight at 393 K and calcined at 823 K for 4 h.

2.3. Characterization

2.3.1. X-ray fluorescence spectroscopy

The metal contents of Ni, W, and Ti were determined on a ZSX100e X-Ray fluorescence analyzer.

2.3.2. X-ray diffraction

X-ray diffraction patterns were recorded on a SHIMADZU-6000 diffractometer, using the CuK_α radiation at 40 kV and 30 mA with a scanning rate of 2°/min.

2.3.3. N_2 physisorption

The BET surface area and pore volume of the supports and oxide form catalysts were determined by N_2 physisorption using a Micromeritics ASAP 2020 automated system. Each sample was degassed at 623 K for 5 h prior to N_2 physisorption.

2.3.4. Infrared spectroscopy

Acid sites and acid type distribution of the oxide form catalysts were determined by infrared spectroscopy (IR) of chemisorbed pyridine. All spectra were recorded on a MAGNA-IR560ESP Fourier-transform infrared spectrometer at a resolution of 0.35 cm^{-1}. The sample degas was carried out at 623 K and 10^{-3} Pa for 4 h prior to the adsorption of pyridine. IR spectra were recorded after subsequent evacuation at increasing temperatures from 473 to 623 K (1 h at each temperature).

2.3.5. Temperature-programmed desorption

NH_3-temperature-programmed desorption (TPD) of the oxide form catalysts were performed by using Quantachrome Autosorb-1, equipped with a QUADSTAR 32-bit quadrupole mass spectrometer (QMS) 200 to monitor the exit gas. A sample of 0.20 g was charged in the quartz tube and heated at a rate of 10 K/min to 773 K for 30 min under N_2 flow before exposure to 100% NH_3 at 298 K for 30 min. The NH_3-TPD spectrum was recorded from 373 to 973 K at the heating rate of 10 K/min after removing weakly adsorbed NH_3 by heating the catalyst to 373 K under pure N_2 flow. The total flow rate of gas was fixed as 30 cm^3/min.

2.3.6. Temperature-programmed reduction

The temperature-programmed reduction (TPR) experiments of the oxide form catalysts were carried out on a Quantachrome Autosorb-1. Prior to the reduction, the catalyst sample in a quartz reactor was pretreated in an O_2 flow of 30 cm^3/min at 573 K for 3 h and cooled down to room temperature. Then the TPR experiment was run in a 10% H_2/Ar (by volume) flow of 30 cm^3/min, heating up to 1273 K at a rate of 5 K/min, with a Quantachrome Autosorb-1-C TCD controller to monitor the exit gas.

2.3.7. Diffuse reflectance spectra

Diffuse reflectance spectra (DRS) of the oxide form catalysts were recorded in the 350–800 nm range using the corresponding support as reference on a Hitachi U-4100 Spectrophotometer.

2.3.8. Laser Raman spectra

Laser Raman spectra of the oxide form catalysts were recorded in the range of 200–1200 cm^{-1} under ambient conditions on a computer-controlled Renishaw microscopic confocal Raman spectrometer, model RM2000, using the 514.5 nm line from a Spectra Physics model 165 Ar ion laser as the exciting source. The spectra shift width was typically 1 cm^{-1}, and laser source powers at the sample were ca. 4.7 mW.

2.3.9. Catalytic activity evaluation

The HDS of 4,6-DMDBT was evaluated in a fixed-bed flow reactor under the conditions: 4.0 MPa, 553 K, the catalyst loading of 0.60 g, 0.66 wt% 4,6-DMDBT in decane as the model feed, the feed flow rate of 6.85 mL/h, H_2/Oil ratio of 500 v/v. The catalysts were presulfied *in situ* with the sulfiding feed of 10 vol% CS_2 in decane, 4.0 MPa and 573 K. After steady-state conditions were reached, the liquid effluents were periodically collected. And the total sulfur content in the feed (S_{feed}) and products ($S_{product}$) was measured by using a LC-4 coulometric sulfur analyzer. Finally, the HDS activity of 4,6-DMDBT was calculated as follows:

$$\text{HDS conversion}(\%) = [(S_{feed} - S_{product})/S_{feed}] \times 100.$$

The compounds in the liquid effluents were identified by Finnigan Trace GC/MS with a Trace Ultral gas chromatograph using a HP-5MS (30×0.25×0.25) capillary column and a flame ionization detector.

3. Results and discussion

3.1. X-ray diffraction

The XRD patterns of the correspondingly calcined supports and catalysts were shown in figures 1 and 2. The XRD patterns of the composite support AETS and Al_2O_3–TiO_2 exhibit the characteristic peaks of ETS-10 and TiO_2 (anatase), respectively, which indicates their stable embedding in alumina matrix. After the impregnation of Ni and W, no obvious metal oxides peaks are found in the XRD patterns of NiW/AETS, NiW/Al_2O_3–TiO_2 and NiW/Al_2O_3, although the characteristic peaks of ETS-10 and TiO_2 weaken to some extent, due to the dilution effect or partial breakdown of ETS-10 and TiO_2 structure caused by the metal oxides [11].

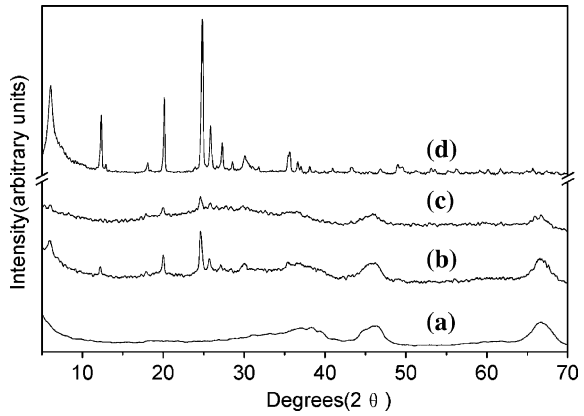

Figure 1. X-ray diffraction patterns of (a) Al_2O_3; (b) AETS; (c) NiW/AETS and (d) ETS-10.

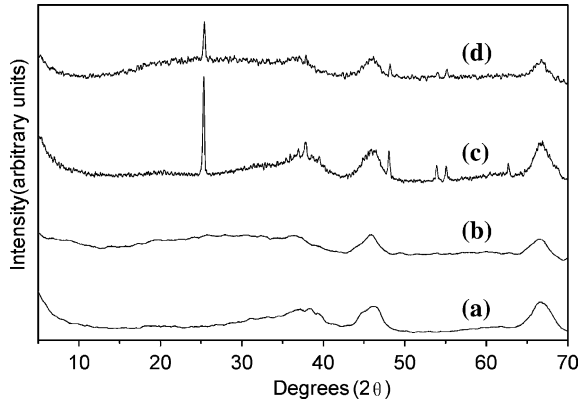

Figure 2. X-ray diffraction patterns of (a) Al_2O_3; (b) NiW/Al_2O_3; (c) Al_2O_3–TiO_2 and (d) NiW/Al_2O_3–TiO_2.

3.2. N_2 physisorption

The textural properties of the samples listed in table 1 indicate that the incorporation of ETS-10 into alumina remarkably enlarges the surface area but slightly decreases the total volume of both the composite support and the related catalyst, which attributed to larger surface area but lower pore volume of ETS-10 [9] than that of Al_2O_3 correspondingly.

3.3. Infrared spectroscopy

The results of the acid sites and acid type distribution of NiW/Al_2O_3 and NiW/AETS were shown in table 2. From the data, it can be clearly seen that NiW/AETS owns less total L type acid sites (pyridine desorption temperature at 473 K), especially less strong-strength L type acid sites (pyridine desorption temperature at 623 K) than NiW/Al_2O_3. But most importantly, there are still a certain amount of B type acid sites (pyridine desorption temperature at 473 K) on the surface of NiW/AETS, due to that ammonium-exchanged ETS-10 has some B type acid sites [9], which could probably contribute to the isomerization of refractory 4,6-DMDBT into more reactive compounds so as to enhance the HDS activity [5,7], but avoid over-cracking or deactivation effectively.

Table 1
BET surface areas and pore volumes of the samples

Sample	Surface area (m^2/g)	Pore volume (cm^3/g)
Al_2O_3	281	0.53
AETS	318	0.50
NiW/Al_2O_3	193	0.35
NiW/AETS	215	0.31

3.4. Temperature-programmed desorption

NH_3-temperature-programmed desorption (TPD) of the oxide form catalysts were shown in figure 3. It was obvious that the shapes of the corresponding desorption curves were very similar, suggesting similar distributions of acidic sites over the catalysts. In contrast, the NH_3 desorption peaks of NiW/AETS shifts to lower temperature slightly in comparison with those of NiW/Al_2O_3 or NiW/Al_2O_3–TiO_2, ascribed to NiW/AETS owning less strong acid sites compared with NiW/Al_2O_3, which has been proven by the results of pyridine-IR desorption in table 2. The NH_3-TPD experimental results further confirm that NiW/AETS containing ETS-10, unlike previously reported acidic molecular sieves [5,7], will not cause over-cracking.

3.5. Temperature-programmed reduction

The TPR profile of NiW/Al_2O_3 in figure 4 shows two peaks at 887 and 1229 K, respectively. Noticeably, the steady increase in the baseline and broad peaks of its TPR profile, may indicate the reduction of dispersed nickel and tungsten species of various reducibility due to the strong interaction with alumina [12,13]. In contrast, the TPR profile of NiW/AETS shows two sharp peaks at 860 and 1098 K, notably shifting to lower temperatures correspondingly. It can be properly explained that the incorporation of ETS-10, especially attributed to its titanosilicate framework, could play a beneficial role in suppressing the most reactive hydroxyl groups responsible for the metal oxides species interacting strongly with alumina support, because of their intimate contact obtained by making ETS-10 dispersed uniformly in alumina matrix. Furthermore, it could also relieve the polarizing effect of aluminium ions of the alumina support on metal ions in the catalysts, which leads to substantial improvement on metal–support interactions and causes easier reduction of nickel and tungsten [5,6,12,13].

3.6. Diffuse reflectance spectra

As the DRS spectra shown in figure 5, two visible peaks at 590 and 630 nm, are found, respectively, ascribed to the presence of tetrahedrally coordinated

Table 2
Total acid and acid type distribution of NiW/Al_2O_3 and NiW/AETS

Sample	473 K		623 K	
	B acid (mmol/g)	L acid (mmol/g)	B acid (mmol/g)	L acid (mmol/g)
NiW/Al_2O_3	–	0.11	–	0.070
NiW/AETS	0.011	0.072	–	0.019

Ni^{2+} ions in $NiAl_2O_4$ in the spectra of NiW/Al_2O_3 and NiW/Al_2O_3–TiO_2, consistent with the previous results [14–16]. In contrast, no such obvious peaks exist in the spectra of NiW/AETS. But it can be clearly seen that the band around 420 nm, characteristic of octahedrally coordinated Ni^{2+} ions, shifts to higher wavenumbers with the introduction of ETS-10 into alumina, indicating an enhanced incorporation of nickel with tungsten producing Ni–W–O species [15,16]. Therefore, it can be safely concluded that the Ni^{2+} ions are liable to be octahedrally coordinated on the composite support AETS due to the modifying effects of titanosilicate framework of ETS-10 on alumina, which effectively impedes the diffusion of Ni ions into the alumina lattice [15,16].

3.7. Laser Raman spectra

The LR spectra of the oxide form catalysts were shown in figure 6. In the LR spectra of NiW/Al_2O_3, a noticeable band at 975 cm^{-1} was found. However, the corresponding peak shifted to 978 cm^{-1} in the LR spectra of NiW/AETS, indicating that the degree of polymerization of tungsten species is increased [17–19]. It could be ascribed to the surface characteristic of composite support AETS favoring the formation of octahedrally coordinated polymeric tungsten species, which has been reported to interact with support weakly, contributing to easier reducibility (as shown in figure 4) and higher activity [17–20]. In contrast, the band around 970 cm^{-1} in the LR spectra of NiW/Al_2O_3–TiO_2 was obscured but still noticeable because of the presence of strong bands characteristic of TiO_2 (anatase) [17,18,21].

3.8. Catalytic activity evaluation

The HDS of 4,6-DMDBT results illustrated in figure 7 indicate that NiW/AETS exhibits the highest HDS activity, owning an increase of 9% and 7% in HDS conversion, compared with NiW/Al_2O_3 and NiW/Al_2O_3–TiO_2, respectively. Notably, the compounds distribution of the liquid effluents obtained over NiW/AETS shows no obvious difference from that of NiW/Al_2O_3 according to the GC-MS chromatograms,

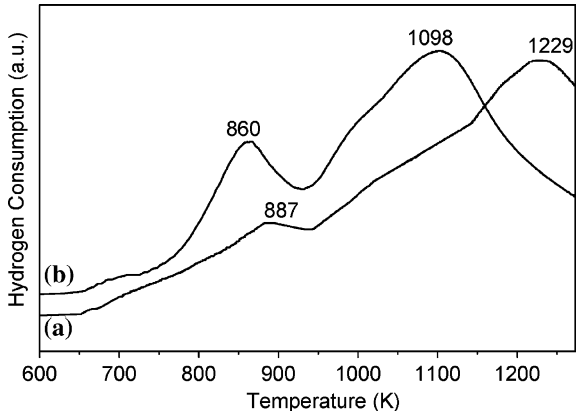

Figure 4. TPR profiles for (a) NiW/Al_2O_3 and (b) NiW/AETS.

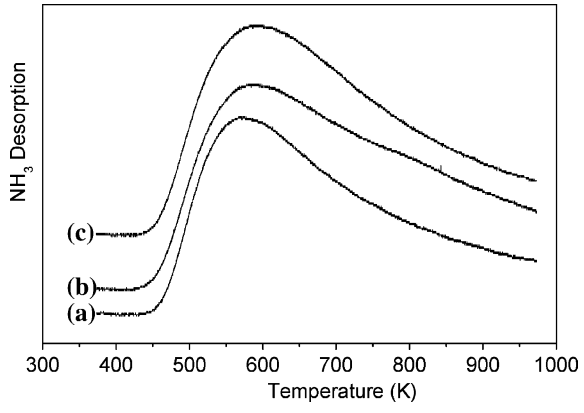

Figure 3. NH_3-TPD spectra of (a) NiW/AETS; (b) NiW/Al_2O_3 and (c) NiW/Al_2O_3–TiO_2.

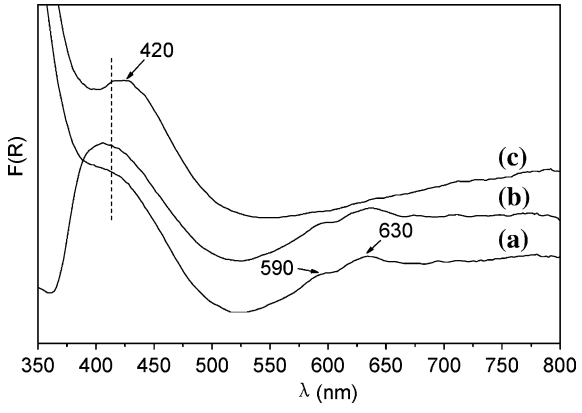

Figure 5. DRS spectra of (a) NiW/Al_2O_3; (b) NiW/Al_2O_3–TiO_2 and (c) NiW/AETS.

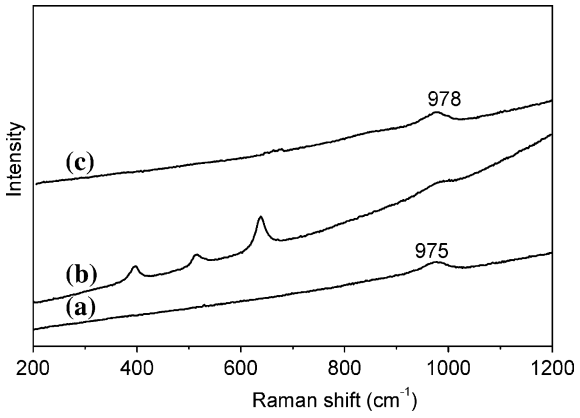

Figure 6. Laser Raman spectra of (a) NiW/Al_2O_3; (b) NiW/Al_2O_3–TiO_2 and (c) NiW/AETS.

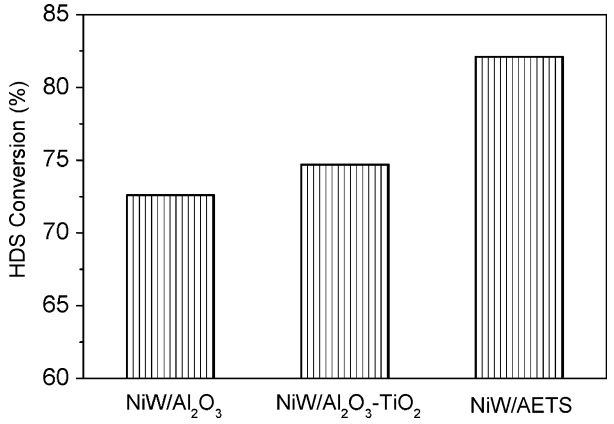

Figure 7. Comparison of the HDS activities of NiW/Al_2O_3, NiW/Al_2O_3–TiO_2 and NiW/AETS.

without much overcracking products formation, due to its moderate acidity as confirmed by the results of Py-IR and NH_3-TPD.

Therefore, the marked enhancement in HDS activity of NiW/AETS can be explained as follows. Firstly, the presence of a certain amount of B type acid sites of moderate acid strength on NiW/AETS could partly increase the HDS activity. Secondly, the impeding formation of inactive nickel spinel as confirmed by DRS spectra in figure 5, favors the promotion effect of nickel on tungsten; Thirdly, the increased degree of polymerization of tungsten species as characterized by LR spectra in figure 6, according to the results reported by the previous literature [20,22], maybe facilitated the formation of the precursor of active sites (Ni–W–S species) for HDS.

4. Conclusion

NiW/AETS shows remarkably higher activity in HDS of 4,6-DMDBT compared with NiW/Al_2O_3 or NiW/Al_2O_3–TiO_2. It can be reasonably attributed to the advantages resulting from the modulation effects of titanosilicate framework of ETS-10 on alumina. Firstly, the incorporation of ETS-10 into alumina considerably improves the reducibility of metal oxides. Secondly, the presence of a certain amount of B type acid sites of moderate acid strength on NiW/AETS could partly increase the HDS activity. Thirdly, the impeding formation of inactive nickel spinel and the increased degree of polymerization of tungsten species, probably facilitated the promotion effect of nickel on tungsten or the formation of the precursor of active sites for HDS, leading to a considerable enhancement in HDS activity.

Acknowledgments

The authors gratefully acknowledge the funding of this project by PetroChina, NSFC (ID 20276039) and MOST "973" Project of China (2004CB217806).

References

[1] A.J. Hernández-Maldonado and R.T. Yang, J. Am. Chem. Soc. 126 (2004) 992.
[2] R.T. Yang, A.J. Hernández-Maldonado and F.H. Yang, Science 301 (2003) 79.
[3] N.A. Dhas, A. Ekhtiarzadeh and K.S. Suslick, J. Am. Chem. Soc. 123 (2001) 8310.
[4] S.K. Bej, S.K. Maity and U.T. Turaga, Energ. Fuel 18 (2004) 1227.
[5] M. Breysse, P. Afanasiev, C. Geantet and M. Vrinat, Catal. Today 86 (2003) 5.
[6] G.M. Dhar, B.N. Srinivas, M.S. Rana, M. Kumar and S.K. Maity, Catal. Today 86 (2003) 45.
[7] G. Pérot, Catal. Today 86 (2003) 111.
[8] A. Liepold, K. Roos, W. Reschetilowski, Z. Lin, J. Rocha, A. Philippou and M.W. Anderson, Micropor. Mater. 10 (1997) 211.
[9] H. Li, B. Shen, X. Wang and S. Shen, Catal. Lett. 99 (2005) 165.
[10] X. Yang, J.L. Paillaud, H.F.W.J. van Breukelen, H. Kessler and E. Duprey, Micropor. Mesopor. Mat. 46 (2001) 1.
[11] S. Bendezú, R. Cid, J.L.G. Fierro and A.L. Agudo, Appl. Catal. A 197 (2000) 47.
[12] C.H. Kim, W.L. Yoon, I.C. Lee and S.I. Woo, Appl. Catal. A 144 (1996) 159.
[13] B. Scheffer, P. Molhoek and J.A. Moulijn, Appl. Catal. A 46 (1989) 11.
[14] E. Olguin, M. Vrinat, L. Cedeño, J. Ramirez, M. Borque and A. López-Agudo, Appl. Catal. A 165 (1997) 1.
[15] P. Atanasova and T. Halachev, Appl. Catal. A 108 (1994) 123.
[16] B. Scheffer, J.J. Heijeinga and J.A. Moulijin, J. Phys. Chem. 91 (1987) 4752.
[17] L. Salvati Jr., L.E. Makovsky, J.M. Stencel, F.R. Brown and D.M. Hercules, J. Phys. Chem. 85 (1981) 3700.
[18] A. Gutiérrez-Alejandre, J. Ramírez and G. Busca, Langmuir 14 (1998) 630.
[19] N. Kunisada, K.-H. Choi, Y. Korai, I. Mochida and K. Nakano, Appl. Catal. A 269 (2004) 43.
[20] D. Li, A. Nishijima, D.E. Morris and G.D. Guthrie, J. Catal. 188 (1999) 111.
[21] J. Ramírez, G. Macías, L. Cedeño, A. Gutiérrez-Alejandre, R. Cuevas and P. Castillo, Catal. Today 98 (2004) 19.
[22] C.J. Song, C. Kwak and S.H. Moon, Catal. Today 74 (2002) 193.